JPE 12-1-9

http://dx.doi.org/10.6113/JPE.2012.12.1.67

Noise Lowering for a Large Variable Speed Range Use Permanent Magnet Motor by Frequence Shift and Structural Response Evaluation of Electromagnetic Forces

Masanori Arata†, Norio Takahashi*, Masafumi Fujita*, Motoyasu Mochizuki*, Takashi Araki**, and Takashi Hanai**

†* Toshiba Corporation, Yokohama, Japan
** Toshiba Industrial Products Manufacturing Co., Yokohama, Japan

Abstract

According to electrical output up rating of a permanent magnet motor and request to operate for a large variable speed range, resonance between structural natural vibration and electromagnetic force inside the motor can take place and make noise. This paper describes the mechanism of a resonance between them and noise lowering procedure by frequency shift when they are applied to the reluctance torque largely employed new motor named Permanent magnet Reluctance Motor (PRM).

Key Words: Electric Drive, Electromagnetic force, Hybrid Electric Vehicles, Noise

I. INTRODUCTION

Permanent Magnet (PM) motors using NdFeB magnets having high power and high efficiency are applied to many drive systems these days. The flux-weakening for constant-power operation to control the air-gap flux and the terminal voltage constant allows PM motors to operate at a speed range about 1:3 [1], [5].

Those wide speed range operation can arise a resonance between structural natural vibration and electromagnetic force inside the motor. And it results in poor silence and it is impossible to operate beyond the resonant point in some case.

Silent operations are desirable and important for the motor driving systems of an electric vehicle (EV) and a hybrid electric vehicle (HEV). But it is more difficult for them because they must operate at variable speed ranges up to 1:5. So they have more possibility to meet more resonant points in comparison with other applications [2]–[5].

II. PRM MOTOR

The flux weakening method for constant-power operation enlarges the operation range of various Permanent Magnet (PM) motors (Fig. 1). But even for an Interior Permanent magnet Motor (IPM) [2], [10], its operation speed range at a constant-power without voltage booster circuit about 1:3, as shown in Fig. 2. And it results in poor efficiency by increase of the flux weakening current [6], [7] and iron losses in those high-speed regions. In addition, there is still a possibility for breakdowns of capacitors and/or power devices of an inverter due to excess voltage in case the lost of flux-weakening control.

The authors have been developing the Permanent magnet Reluctance Motor (PRM) to resolve those defects of the IPM by largely employing the reluctance torque by changing the magnet position and magnetic circuit design. Increase of reluctance torque leads to decrease of permanent magnet amounts and smaller back EMF. They allow a large variable speed range over 1:5, smaller flux weakening current and higher efficiency at high speed operating region. [1], [2], [10] Fig. 3 shows a typical cross section of the PRM and its variety. They are both possible to create magnetic flux flow controller increasing the difference d-axis and q-axis reactance by cutting an air holes inside a rotor and by setting a groove outside a rotor.

Fig. 4 shows typical structure of PRM. After adjustment between motor performance and noise, it delivers maximum torque of 210Nm and maximum output of 65kW. It can operate until 13500rpm at almost constant power.

Fig. 5 shows typical a torque versus rotating speed characteristic. The PRM is a powerful, compact motor and suitable to a variable speed drive.

Manuscript received Sep. 19, 2011; revised Dec. 14, 2011
Recommended for publication by Associate Editor Jung-Ik Ha.
† Corresponding Author: masanori.arata@toshiba.co.jp
Tel: +81-45-510-6624, Fax: +81-45-500-1973, Toshiba Co.
* Toshiba Corporation, Japan
** Toshiba Industrial Products Manufacturing Co., Japan

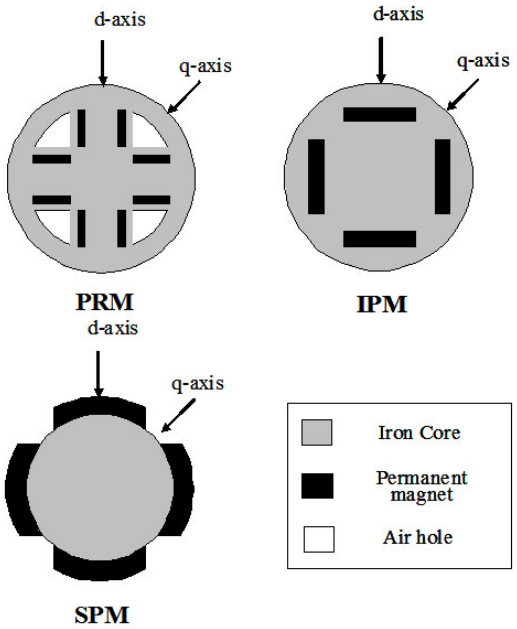

Fig. 1. Rotor Configurations of PM Motors.

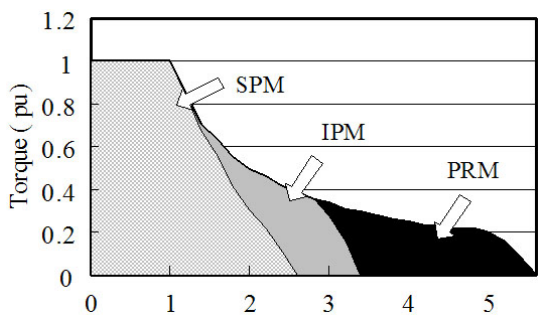

Fig. 2. Performance of Motors at Variable speed.

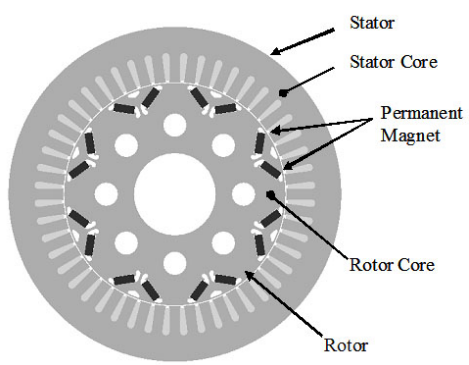

(a) An example of cross section of the PRM.

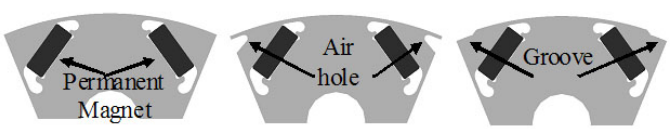

(b) Rotor structure variety (pole part).

Fig. 3. Structure of PRM.

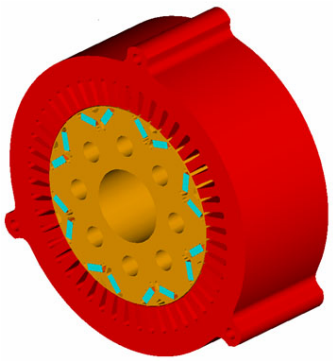

Fig. 4. PRM Structure for SUV.

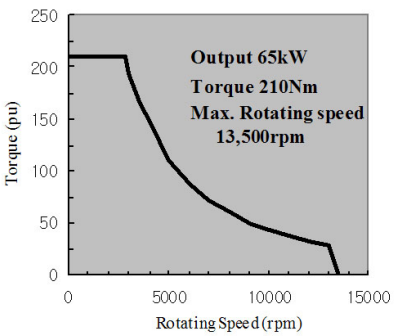

Fig. 5. PRM torque characteristics For SUV.

III. NOISE LOWERING OF PRM

Original PRM for Hybrid SUV use has 8 poles in the rotor and 36 slots in the stator to maximize its torque and output power considering motor efficiency and producibility. When it delivered required torque along the specifications rotating speed range, it generated large noise around 7000 rpm. For mass production, this noise had to be low without degrading the motor performance.

A. Noise and core natural frequence measurements

Noise and vibration frequency and vibration mode were measured to identify the root cause of large noise around 7000 rpm. Fig. 6 shows over all audible noise measured on the microphone at 10cm from motor frame delivering the required torque plotted in the figure 3. Audible noise characteristic at no load condition is fairly flat and low. It becomes noisy from 4000rpm to 11000rpm, especially around 7000rpm.

Waterfall analysis is conducted to identify the major harmonics of the noise. Fig. 7 shows the waterfall plot of original PRM noise measure by the same procedure of Fig. 6.

There are some harmonics such as 24th, 40th, and so on. But the 32nd order noise is larger than other component and largest around 7000 rpm.

Fig. 8 also shows the waterfall plot of original PRM stator core vibration measured with an acceleration sensor directly attached to the core through small hole of the motor frame. In the core vibration, the 32nd order noise is also larger than other component and also largest around 7000 rpm. From noise and vibration characteristics, the root cause of noise around 7000rpm reflected on the core and the motor frame vibration.

Natural frequence and its mode of the stator core were measured at support free condition.

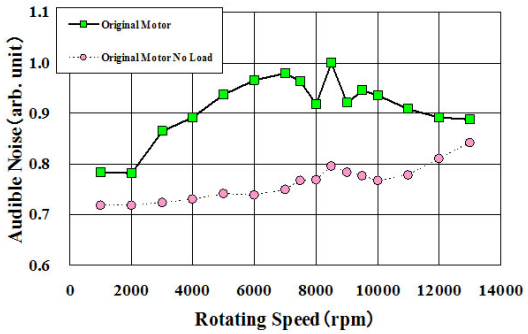

Fig. 6. Over all audible noise characteristics of PRM.

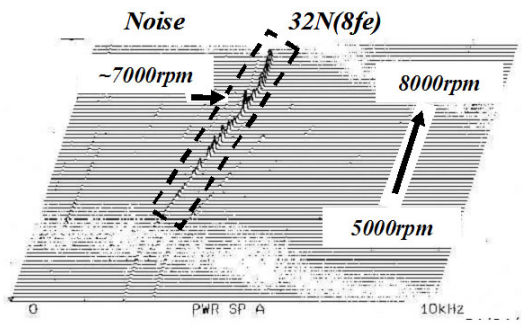

Fig. 7. Noise Waterfall Plot of PRM.

The core without stator coil and vanish was sit on a rubber sheet and hammered by an impulse hammer.

Fig. 9 and Fig. 10 show the measured the stator natural frequence and its mode.

At 750Hz, the Core has cocoon like shape K=2 vibration mode. Also, it has triangle like shape K=3 at 2300Hz. At 3500Hz, its vibration mode looks like clover shape; K=4. And it has uniform vibration mode K=0 at 5325Hz.

The frequence of the 32nd noise and vibration is about 3700Hz at rotating speed of 7000rpm. If excitation forces has 4th order harmonics in space, a resonance between the force and a natural frequence will take place.

B. Electromagnetic Force Evaluation and Analysis

An excitation force potentially arises from electro-magnetic force inside the motor. The original design has 8 poles in the rotor and 36 slots in the stator. Slot numbers per phase per pole is 1.5, fractional slots design. In this design, when north poles of the rotor align stator coils with five teeth, the south poles face the stator coils with four teeth as shown in Fig. 11. Consequently electromagnetic force at north poles is relatively strong and the force at south poles is weak. So there exist forces of 4th order harmonics in space; clover shape K=4.

2 dimensional finite element analyses (FEA) are conducted to confirm above electromagnetic force diagram and to evaluate electromagnetic force quantitatively in space and time. Fig. 12 shows a FEA model in wire frame style. It is a one-fourth model using its symmetry. It also shows an electromagnetic force distribution. Inwards arrows on the teeth present electromagnetic force acting the stator. Force on the every tooth are different each other and it is very large on some teeth. K=4 electromagnetic force arising from fractional stator slot number design and the K=4 mode core natural

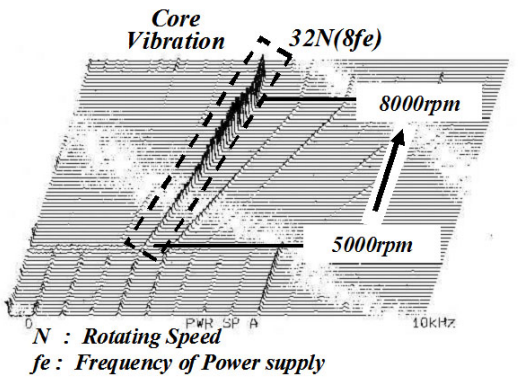

Fig. 8. Stator Core Vibration Waterfall Plot of PRM.

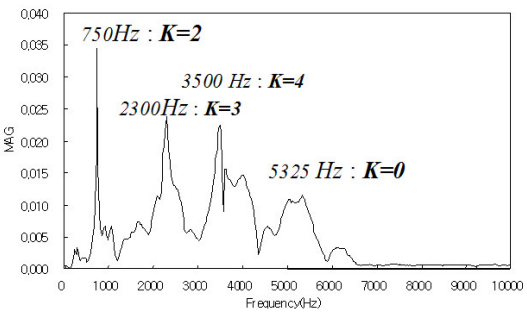

Fig. 9. Stator Core natural frequence of PRM.

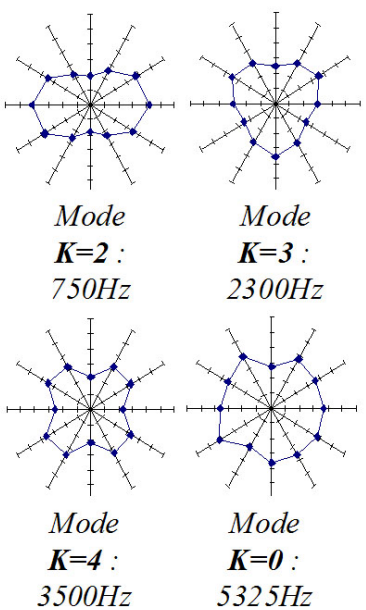

Fig. 10. Stator Core natural frequence vibration mode of PRM.

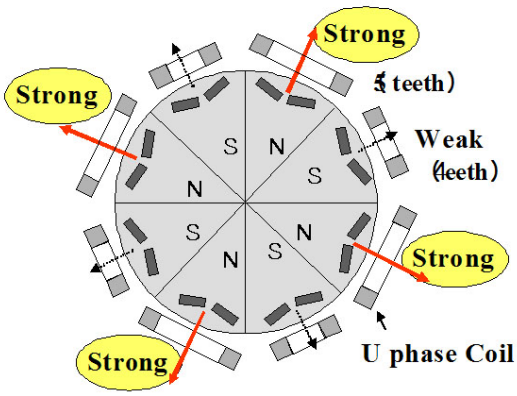

Fig. 11. Stator Core natural frequence vibration mode of PRM.

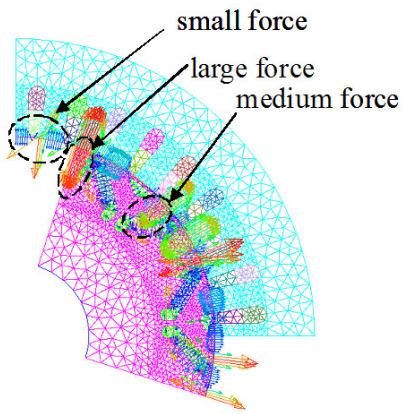

Fig. 12. Electromagnetic Force Distribution of PRM with 8-pole Rotor and 36 slots Stator.

frequency. Electromagnetic force acting on the tooth node in the FEA model is separated into every time harmonics by the Discrete Fourier transform method. [12] Then the every time harmonics of electromagnetic force acting each tooth is obtained integrating the corresponding time harmonics of the node force. Fig. 13 shows electromagnetic force of each tooth separated into every time harmonics for 360 electric degrees in above FEA model. Synchronous component becomes DC component and expressed 0th in Fig. 13 and it is largest. One cycle distribution in Fig. 13 is mode K=4 because the FEA model is a one fourth model. According from the Fig. 13, the 8th time harmonics is the one cycle distribution and the mode K=4. The 8th harmonics becomes 32nd harmonics of a rotating speed because this motor is 8 poles. Those force distribution; mode K=4 and its frequence meet the observed core vibration shown in the Fig. 8. The root cause of noise and vibration around 7000rpm was identified to be a resonance between mode K=4 electromagnetic force arising from fractional stator slot number design and the K=4 mode core natural frequency.

C. Electromagnetic force analysis for alternative design

Electromagnetic force analysis and noise evaluation are outlined here with an example of 8 poles 48 slots design. Fig. 14 shows a FEA model in outline style. It is also a one fourth model using its symmetry. It shows an electromagnetic force distribution with flux line contour. Inwards arrows on the teeth also present electromagnetic force acting the stator.

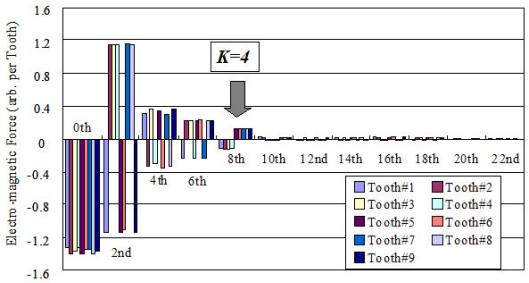

Fig. 13. Electromagnetic Force Distribution of PRM with 8-pole Rotor and 36 slots Stator.

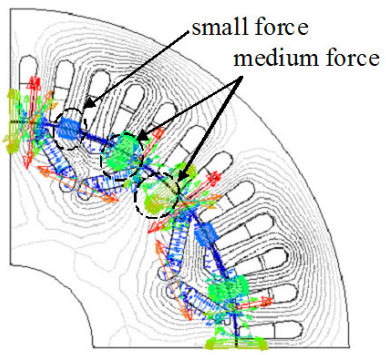

Fig. 14. Electromagnetic Force Distribution of PRM with 8-pole Rotor and 48 slots Stator.

Force on the every tooth in Fig. 14 becomes almost same level comparing with Fig. 12.

Fig. 15 shows electromagnetic force of each tooth separated into every time harmonics for 180 electric degrees in above FEA model. The 10th time harmonics of electromagnetic force becomes mode K=8 in space and lower time harmonics than 10th show distribution of higher mode in space. On the contrary, higher time harmonics than 12th do not shows lower mode force distribution. The 12th harmonics of electromagnetic force in time has mode K=0 distribution in space. It can resonate with K=0 core natural frequency. The 12th harmonics is 48th harmonics of a rotating speed. It encounter K=0 core natural frequency around 6650rpm because K=0 core natural frequency is 5325Hz. So noise can arise around 6650rpm in 8 poles 48 slots design.

Same force analysis is conducted on the 6 poles 36 slots design and other alternatives. Calculated force values are also used in core response and noise estimation analysis. Fig. 16 shows an example of force calculation for another alternative design, 8 poles 24 slots design. There are some time harmonics have K=0 space distribution. It encounters core natural frequency at some points. Resonant point evaluations are discussed later.

D. Pole and Stator slot Number evaluation

The core has some natural frequencies within operation range as shown in Fig. 9. It is impossible to sweep off every natural frequence from operating range in this application. The responses between electromagnetic force and natural frequence are calculated and evaluated by changing rotor pole number and stator slot number to reduce the motor noise. The comparatively higher order vibration mode is excited

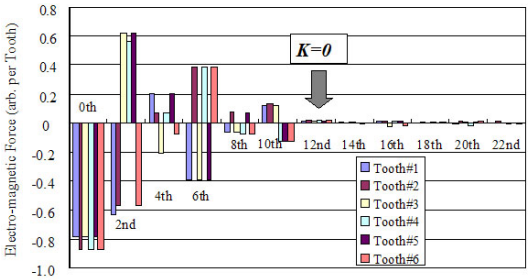

Fig. 15. Electromagnetic Force Distribution of PRM with 8-pole Rotor and 48 slots Stator.

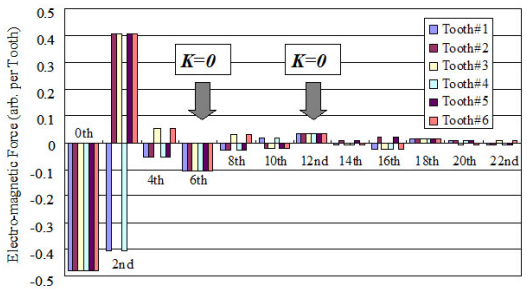

Fig. 16. Electromagnetic Force Distribution of PRM with 8-pole Rotor and 24 slots Stator.

by the electromagnetic force arising from fractional stator slot number design. Integral slots number per phase per pole designs are chosen excepting 10 poles 45 slots design to lower the motor noise. It is included because K=5 mode core natural frequency is not clearly observed as shown in Fig. 9. 8 poles designs with 48 slots and 24 slots, 6 poles designs with 36 slots, and 10 poles design with 45 slots and 30 slots are considered for this evaluation. Electromagnetic force possibly causing the noise and its expecting rotating speed are examined. Candidate electromagnetic force which cause noise is changed to mode K=0 from K=4 and expecting rotating speed are about 6600rpm for 8 poles design, about 8800rpm for 6 poles design, and 10000rpm for 10 poles design. Rotating speeds which encounter the resonance between electromagnetic force and core natural frequence are shown from Fig. 17 to Fig. 19 for every pole number.

Electromagnetic forces possibly causing the noise, and estimated noise are summarized in Table I. Estimated noise is almost same level and lower in 8 poles 48 slots design and 6 poles 36 slots design. Considering maximum delivered torque, torque ripple, Candidate designs are focused above two designs.

TABLE I
ELECTROMAGNETIC FORCE AND NOISE FOR ALTERNATIVE DESIGNS

Alternative Design	8-pole 48-slot	8-pole 24-slot	6-pole 36-slot	10-pole 45-slot	10-pole 30-slot
Electro-magnetic Force (arb. Per Tooth)	0.0044	0.058	0.0058	0.0084	0.058
Total electro-magnetic Force (arb.)	0.21	1.39	0.20	0.37	1.74
Audible Noise (arb.)	0.93	1.07	0.92	1.0	1.09

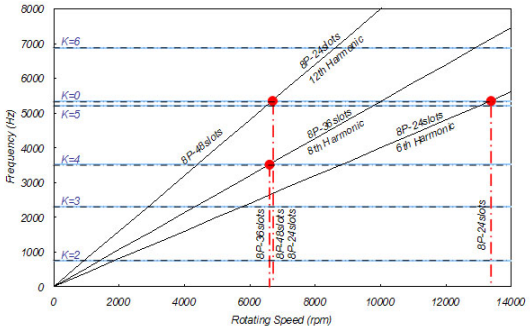

Fig. 17. Resonance rotating speed for 8-pole design.

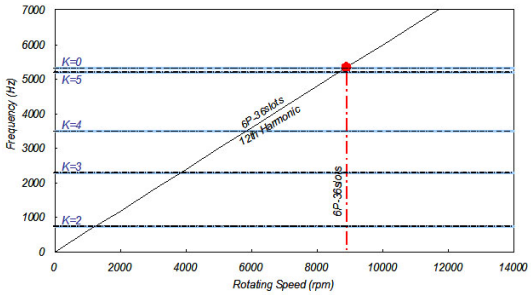

Fig. 18. Resonance rotating speed for 6-pole design.

E. Vibration and response analysis

An analytical stator model for response is shown in Fig. 20. It is an example of FEA mesh with 48 slots. 13950 nodes and 8921 elements are in that model. Stator coils are considered as added mass in the calculations.

The stator is fixed to a motor fame at three tab parts with bolts. Those tab parts and the frame are assembled with clearance fit in the actual motor. So force and moment transmissions are estimated to be poor. One tab part is fixed in calculations as a boundary condition. Axial stiffness is determined referring to experiences of similar size industrial motor stator cores.

Commercial software I-dears calculates vibration mode and deformations. Fig. 21 shows vibration modes on the analytical model. Necessary modes are proved to be excited in the model. It shows the model can simulate the motor actual vibration by comparing Fig. 10 and Fig. 20.

Fig. 22 shows response analysis results around the stator core natural frequence. Fig. 22(a) shows vibration response of 8 poles 36 slots design at 3680Hz when the stator core is excited with electromagnetic force calculated by above section.

The stator vibrates at K=4 mode and its corresponding rotating speed is 6900rpm. So this response model well simulates the core vibration during the PRM motor operation.

Fig. 22(b) also shows vibration response of 8 poles 48 slots design at 5160Hz when it is excited same ways. The stator vibrates at K=0 mode and its corresponding rotating speed is 6450rpm.

In case of 6 poles 36 slots design, the stator vibrate at K=0 mode with frequence 5670Hz as shown in Fig. 21(c). Its corresponding rotating speed is 9450rpm.

Vibration mode and frequence of 8 poles 48 slots are different from those of 8 poles 36 slots. But the resonant rotating speed are very close each other. So the noise evaluation based

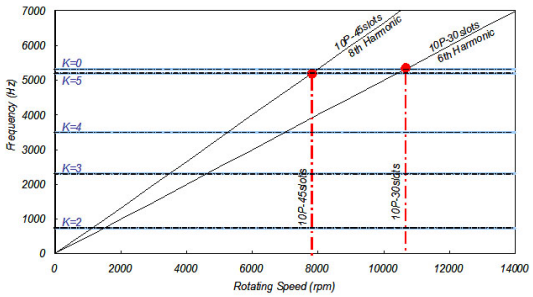

Fig. 19. Resonance rotating speed for 10-pole design.

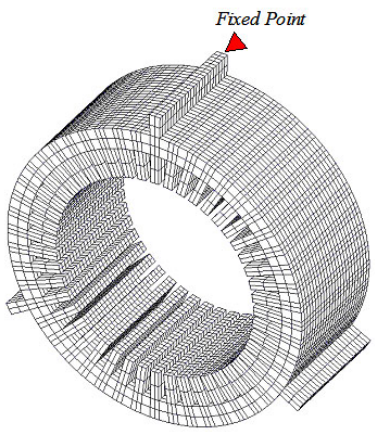

Fig. 20. PRM Analytical Model for Response to Electromagnetic Force.

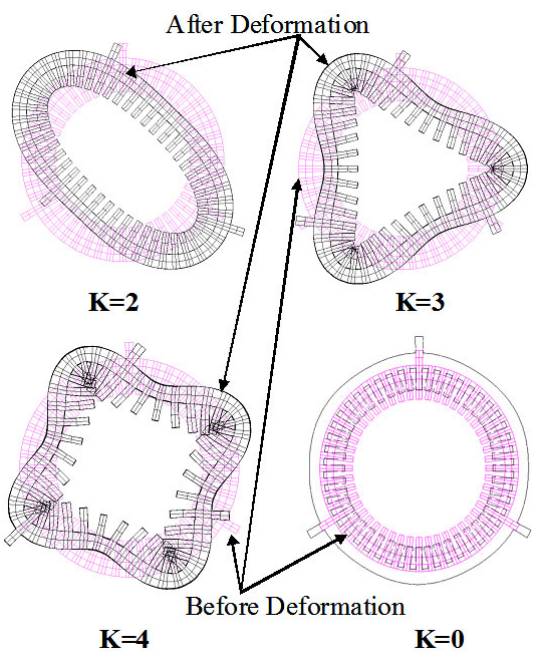

Fig. 21. Vibration Mode on Analytical Model for Response.

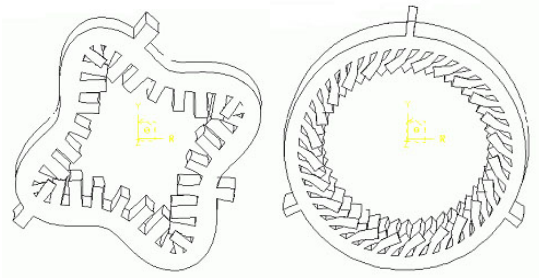

(a) 8P-36slots 3680Hz. (b) 8P-48slots 5160Hz.

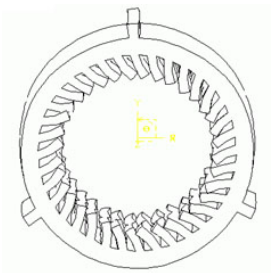

(c) 6P-36slots 5670Hz.

Fig. 22. Displacement of response analysis of 48 slots design and 36 slots design.

on those response analyses is important to judge which is better.

F. Noise evaluation

Vibration acceleration is calculated based on above response analysis. Noise is estimated by multiplying a noise coefficient to the acceleration. This coefficient is adjusted at maximum noise of original design; 8 poles 36 slots. Using that procedure and the coefficient, noises of original design; 8 poles 36 slots, 8 poles 48 slots and 6 poles 36 slots are evaluated and shown in Fig. 23. Calculated noise of original design is increasing from 4000rpm to 10000rpm.

This feature well simulates measured one in Fig. 6. For improved design, 8 poles 48 slots and 6 poles 36 slots are compared. Both designs improve peak noise largely. The 8 poles 48 slots peak noise is about 90% of original design and it is a little better than 6 poles 36 slots one. And for the low rotating speed region; from 4000rpm to 7000rpm, the 6 poles 36 slots is better. Finally, the 8 poles 48 slots was chosen as last design because the peak noise value is better and the maximum torque and motor efficiency are estimated better.

G. Prototype test

A prototype motor as shown in Fig. 24 was built to confirm degree of improvement and evaluate its noise.

Fig. 25 shows 8 pole 48 slots; improved design, noise together with original design. The peak noise became 83% of original design and improved by 10dB. Furthermore, a little noise peak around 4000rpm is expected in improved design by above evaluation in Fig. 23. And it is observed in the prototype test at around 3000rpm. The noise over 10000rpm is estimated increasing in Fig. 23 and this tendency is same in the proto type measurement.

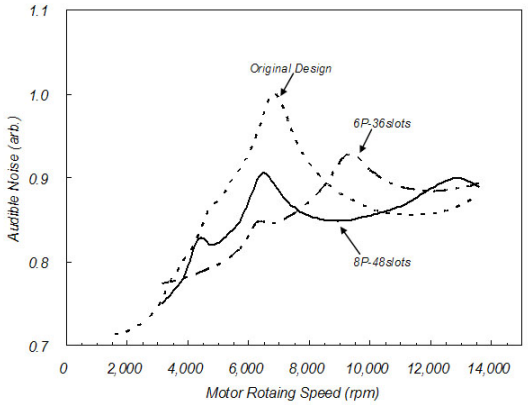

Fig. 23. Estimated each motor noise characteristics based on response analysis.

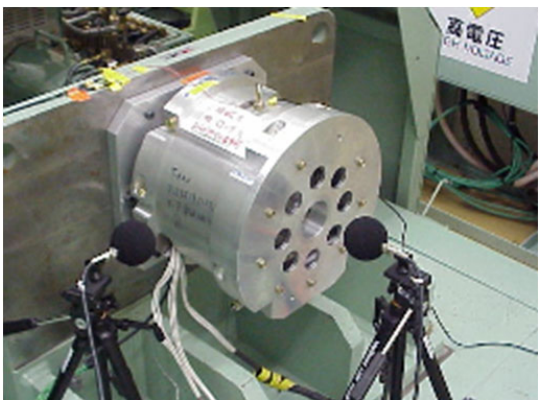

Fig. 24. A prototype motor under measurement.

IV. Conclusions

Noise and vibration frequency and vibration mode were measured to identify the root cause of large noise. Through this measurement and electromagnetic force evaluations, the root cause is a resonance between mode K=4 electromagnetic force arising from fractional stator slot number design and the K=4 mode core natural frequency. Electromagnetic force analysis and noise evaluation are conducted by changing combinations of rotor pole number and stator slot number. Trough those frequency and mode shifting, the estimated noise level of candidate design are compared. 8 pole 48 slots are chosen as final design.

Noise decrease is evaluated and confirmed experimentally. Noise is lowered by about 10dB.

This noise lowering procedure by frequency and mode shift is proved to be effective by applying to a large electrical output and large variable speed range permanent magnet reluctance motor (PRM).

After large improvement in noise, the PRM are applied for a hybrid SUV, a passenger car and a hybrid truck now [2], [3].

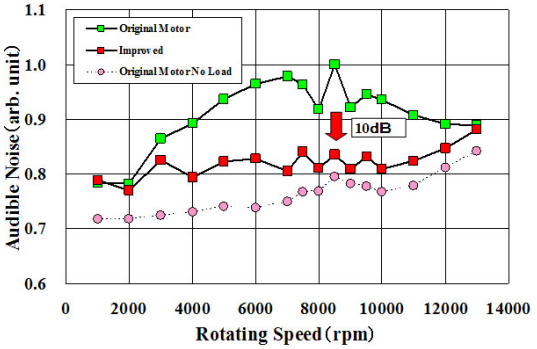

Fig. 25. Improved Over all audible noise characteristics of PRM.

References

[1] T. Teraya, T. Ishikawa, S. Shinnaka, M. Arata, etal., *Motor for Vehicle Use and its Control*, Triceps, Tokyo, 2009.

[2] M. Arata and K. Sakai, "Development of a permanent magnet reluctance motor for automobile use," *Journa of IEEJ*, Vol. 128, No.4, pp.231-234, 2008.

[3] M. Arata, N. Takahashi, K. Sakai, K. Hagiwara, and T. Araki, "Large torque and high efficiency permanent magnet reluctance motor for a hybrid truck," *The 22nd International Battery, Hybrid and Fuel Cell Electric Vehicle Symposium and Expo (EVS22)*, D5, Yokohama, Japan, 2006.

[4] H. Hisada, T. Taniguchi, K. Tsukamoto, K. Yamaguchi, K. Suzuki, M. Iizuka, M. Mochizuki, and Y. Hirano, "AISIN AW New Full Hybrid Transmission for FWD vehicles," *SAE 2005 World Congress*, 2005-01-0277, 2005.

[5] Y. Inakuma, "Electric vehicle (Hybrid vehicle)," *Journal of IEEJ*, Vol. 122, No.11, pp .761-764, 2002.

[6] T. M. Jahns, G. B. Kliman, and T. W .Newmann, "Interior permanent-magnet synchronous motors for adjustable-speed drives," *IEEE Trans. Ind. Appl.*, Vol. IA22, No.4, pp.738-741, Jul. 1986.

[7] W. L. Soong and T. J. E. Miller, "Field-weakening performance of brushless synchronous ac motor drives," *IEEE Proc.-Electr. Power Appl.*, Vol. 141, No. 6, pp.331-334, 1994.

[8] K. Sakai, M. Arata, and T. Tajima, "High-efficiency and high-performance motor for energy saving in systems," *Toshiba Review*, Vol. 55, No. 9, pp. 58-61, 2000.

[9] K. Sakai, K. Hagiwara, and Y. Hirano, "High-power and high-efficiency permanent-magnet reluctance motor for hybrid electric vehicles," *Toshiba Review*, Vol. 60, No.11, pp. 41-45, 2005.

[10] K. Sakai, T. Takahashi, N. Takahashi, M. Arata, T. Tajima, "High efficiency and high performance motor for energy saving in systems," *IEEE Proc. PES. Winter Meeting*, Vol. 3, pp. 1413-1418, Jan. 2001.

[11] M. Arata, M. Mochizuki, and Y. Hirano, "High efficiency and high performance permanent magnet reluctance motor for hybrid electric vehicles," *JSAE Proc. Annual Cong.(Spring)*, 413-20105312, 2010.

[12] A. Kameari, "Local force calculation in 3d fem with. edge elements," *International Journal of Applied. Electromagnetics in Materials 3*, pp.231-240, 1993.

Masanori Arata was born in Tokyo, Japan in 1958. Since 1983, he started working for Toshiba, where he currently belongs to the Power and Industrial Systems Research & Development Center. His research interests are in the areas of a large synchronous electrical machine, a permanent-magnet applied electrical machine. Mr. Arata is a Member of the Institute of Electrical Engineers of Japan.

Norio Takahashi graduated the electrical engineering of the Miyagi technical high school in 1992. He joined Toshiba Corporation in 1992 and has worked on the design and development of Vehicle use electric machines such as rotating machine based on electromagnetic field analysis. Mr. Takahashi is a member of the Institute of Electrical Engineers of Japan.

Masafumi Fujita received the B.E. and M.E. degrees in electrical engineering from Kyoto University in 1989, 1991 respectively. He joined Toshiba Corporation in 1991 and has worked on the design and development of electric machines such as rotating machine based on electromagnetic field analysis. He also received the Master of Philosophy in electrical engineering from University of Bath in 2004. Mr. Fujita is a member of the Institute of Electrical Engineers of Japan and the Institute of Electrical and Electronics Engineers.

Motoyasu Mochizuki was born in 1957. He graduated the Gifu University in 1980. He joined Toshiba Corporation in 1980 and worked on the development and mass-production of electrical power train for vehicles in Automotive Systems Div., where he currently is senior manager of e Driving Systems Engineering Department. Mr. Mochizuki is a member of the Institute of Electrical Engineers of Japan.

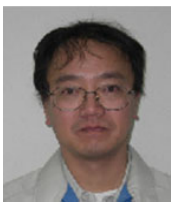

Takashi Araki was born in Mie-Prefecture, Japan, in 1963. He received the B.E. and M.E. degrees in precision engineering from the University of Yamanashi, Japan, in 1988 and 1990 respectively. He joined Toshiba Corporation in 1990, and joined Toshiba Industrial Products Manufacturing Corporation in 2001. He has worked on the design and development of electric machines such as rotating machine. He is currently a quality expert, EV division, Toshiba Industrial Products Manufacturing Corporation. Mr. Araki was a member of the Japan Society for Precision Engineering.

Takashi Hanai was born in Aichi Prefecture, Japan, in1957. He recieved the B.S. and M.S. degrees in electrical engineering from Kyoto University, Japan, in 1979 and 1981, respectively. He joined Toshiba Corporation in1981. He is currently senior manager of Business planning Department, EV division, Toshiba Industrial Products Manufacturing Co. His research interests are in the areas of a induction motor and a permanent magnet motor. Mr. Hanai is a member of the Institute of Electrical Engineers of Japan.